

Original Article

Evaluation of an anatomical syndesmosis classification system

Niklas Bosserhoff¹ , Hannah Gablac² , Michael Hoffmann² 

1. Semmelweis University, Asklepios Campus, Hamburg, Germany.

2. Asklepios Klinik St. Georg, Hamburg, Germany.

Abstract

Objective: To analyze geometric variations of the tibiofibular syndesmosis incisura fibularis to enhance understanding of its anatomical structure and propose a novel anatomical classification system.

Methods: Retrospective analysis of 53 patients who underwent computerized tomography imaging of the ankle. Measurements were taken for various parameters of the incisura fibularis, including length, depth, angle, and fibular engagement. Injury status was taken into consideration.

Results: Based on the incisura angle, a classification was established categorizing the incisura into three types: curved (I_c , angle $< 130^\circ$), normal (I_o , angle 130° – 160°), and shallow (I_s , angle $> 160^\circ$). Correlations between various parameters were identified. Additionally, significant differences in fibular engagement measurements were observed between uninjured (0.96 mm) and injured patients (0.28 mm; $p = 0.017$).

Conclusion: Understanding anatomical variations of the incisura fibularis is crucial for optimizing surgical interventions in syndesmotic injuries. The St. Georg Classification provides a structured approach to guide orthopedic surgeons in creating individualized treatment protocols, reducing the risk of malreduction and improving patient outcomes. Further research is needed to explore the classification's impact on injury patterns and long-term results.

Level of Evidence III; Retrospective comparative study.

Keywords: Ankle; Computed tomography; Fibula; Anatomic variation; Classification.

Introduction

The incisura fibularis, a prominent anatomical feature located on the lateral aspect of the distal tibia, holds a pivotal role in the stability and functionality of the ankle joint^(1,2). This structure is an essential component of the tibiofibular syndesmosis, providing an articulating surface for the fibula and contributing to the structural integrity and biomechanical properties of the syndesmotic joint⁽³⁾.

Comprehensive knowledge of the anatomy of the tibiofibular syndesmosis is critical for orthopedic and trauma surgeons, as ankle injuries are among the most common musculoskeletal injuries^(4,5). Syndesmotic injuries are more common among

athletes, particularly in contact sports⁽⁶⁾, and can account for 12%–32% of ankle sprains in that population^(7–9). Those injuries, also referred to as high ankle sprains, have a longer healing process and a higher risk of long-term complications than lateral ankle sprains⁽¹⁰⁾.

Syndesmotic malreduction is one of the main contributors to long-term complications of high ankle sprains, such as post-traumatic osteoarthritis, limited functional movement, and risk of re-injury^(11,12). Therefore, a well-performed surgery is of utmost importance to achieve an adequate reduction of the injured joint. However, poor reduction is not a rare phenomenon, with malreduction rates ranging between 24% and 52%^(13–15). The variable morphology of the incisura fibularis

The study was performed at the Asklepios Klinik St. Georg, Hamburg, Germany.

Correspondence: Niklas Bosserhoff. Asklepios Campus Hamburg of Semmelweis University Budapest, Lohmühlenstraße 5, 20099 Hamburg, Germany. **Email:** niklas.bosserhoff@semmelweis-hamburg.de. **Conflicts of interest:** none.

Source of funding: none. **Date received:** September 26, 2025. **Date accepted:** December 09, 2025.

How to cite this article: Bosserhoff N, Gablac H, Hoffmann M. Evaluation of an anatomical syndesmosis classification system. *J Foot Ankle.* 2025;19(3):e1950.



has already been described as a risk factor for syndesmotic malreduction, highlighting the importance of understanding its anatomical variations^(16,17).

In this context, the present study aims to contribute to a better understanding of the tibiofibular syndesmosis by providing a geometric analysis of anatomic variations of the incisura fibularis. Additionally, the results of this study aim to define a novel incisura classification system. This knowledge will help orthopedic surgeons and sports physicians develop individualized treatment protocols for syndesmosis injuries.

Patients and methods

The present research was approved by the Ethics and Research Commission. The study population consisted of 53 patients who underwent computed tomography (CT) of the ankle joint at a hospital in Hamburg, Germany, between February and August 2023. Acute fractures affecting the integrity of the incisura fibularis were excluded from this study. However, tibial fractures that had already been treated with open reduction and internal fixation and other fractures (e.g., fibula, talus, calcaneus) were not excluded.

All measurements were performed at the department of radiology of the using the IDS7™ program by Sectra® (Sectra AB, Linköping, Sweden). Variables were assessed in the transverse plane and 10 mm above the tibiotalar joint gap.

Measurements were performed using CT scan images. Figure 1A-G graphically illustrates measurements on the CT sectional plane. Incisura length was measured as the distance between the most prominent edges of the incisura fibularis (also known as intertubercular line, IL)⁽¹⁶⁾. Incisura depth was measured as the perpendicular distance between the deepest point of the incisura and the IL. This angle was defined as the angle between the two lines coming from

the incisura edges to the deepest point of the incisura. The incisura length and incisura angle form a triangle whose area can be calculated using the standard geometrical formula $0.5 \times a \times b$ (a being incisura length, b being incisura depth). This triangle area approximately represents the articular surface of the fibula inside the tibiofibular syndesmosis. This variable describes the perpendicular distance from the IL to the edge of the medial cortex of the fibula. An overlapping of the medial fibular cortex over the IL was considered a positive fibular engagement. Medial fibular cortex not reaching the IL was considered a negative fibular engagement. This length describes the distance between the anterior edge of the incisura and the nearest point of the fibular cortex. Correspondingly, this length describes the distance between the posterior edge of the incisura and the nearest point of the fibular cortex.

Variables fibular engagement, syndesmosis anterior length, and syndesmosis posterior length were unusable if a dislocated fibular fracture was apparent (n = 8).

For some investigations, study population was divided into two groups according to injury status (uninjured and injured).

All procedures performed in this study complied with the ethical standards of the German national research committee, the 1964 Helsinki Declaration and its later amendments, or comparable ethical standards. Existing data was analysed anonymously, therefore, no consent to participate was necessary.

Statistics

Normality of data was tested using the Shapiro-Wilk test. Significance was set at $p < 0.05$. Pearson's Chi-squared test, Wilcoxon rank sum test, Wilcoxon rank sum exact test, and Fisher's exact test were used to compare groups.

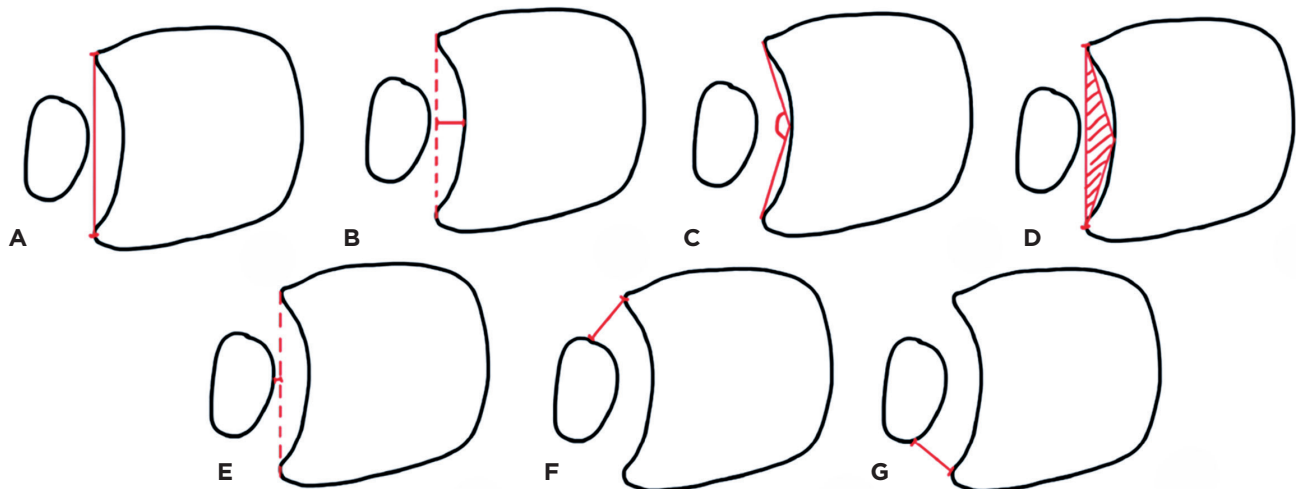


Figure 1. Incisura length (A); incisura depth (B); incisura angle (C); triangle area (D); fibular engagement (E); syndesmosis anterior length; (F) syndesmosis posterior length (G).

Descriptive statistics was applied, and scatterplots were used to graphically represent correlations between variables. Analyses were performed using the program R Core Team (version 4.3.3).

Results

Anatomical variants of the distal tibiofibular syndesmosis were subdivided into three configurations based on measurements of the incisura angle. The incisura angle ranged from 111.8° to 167.5°, with an average angle of 144.60°. The standard deviation (SD) was $\pm 12.01^\circ$.

These three groups are described as follows:

- Curved Incisura fibularis (I_c): every angle $< 130^\circ$ ($n = 3$);
- Normal incisura fibularis (I_o): every angle between 130° and 160° ($n = 44$); and
- Shallow incisura fibularis (I_s): every angle $> 160^\circ$ ($n = 6$).

Figure 2 shows the distribution of the parameter incisura angle in the study population and cutoffs for our novel classification system.

Table 1 shows data for all patients, as well as data for the uninjured and injured subgroups. Twenty-five patients had no tibial or fibular fracture. Fifteen patients underwent surgery with open reduction and internal fixation. The other 13 patients had acute fractures that did not affect the integrity of the incisura fibularis. However, in eight patients, fibular integrity was compromised, thus, in those patients, the three variables fibular engagement, syndesmosis anterior length, and syndesmosis posterior length could not be defined.

Demographic data

The study group consisted of 19 women and 34 men with an average age of 43.28 years (range: 16–84; median: 39). Twenty-eight CT scan images of the right ankle and 25 CT scan images of the left ankle were assessed.

Incisura length

The incisura length ranged from 20.3 mm to 29.0 mm, with an average length of 24.20 mm ($SD \pm 2.28$ mm). Average incisura length of the uninjured group (24.98 mm) was significantly higher than that found in the injured group (23.51 mm) ($p = 0.03$).

Incisura depth

The incisura depth ranged from 1.3 mm to 7.7 mm, with an average depth of 3.79 mm ($SD \pm 1.36$ mm). No correlation could be identified between incisura length and depth (Pearson's correlation coefficient = 0.09).

Incisura angle

Descriptive statistics are mentioned above. There was a strong correlation (Pearson's correlation coefficient = -0.96) between the incisura depth and the incisura angle ($p < 0.001$). The angle did not differ between the subgroups.

Triangle area

The triangle area ranged from 14.63 mm² to 94.71 mm², with an average area of 45.98 mm² ($SD \pm 17.09$ mm²). There was a

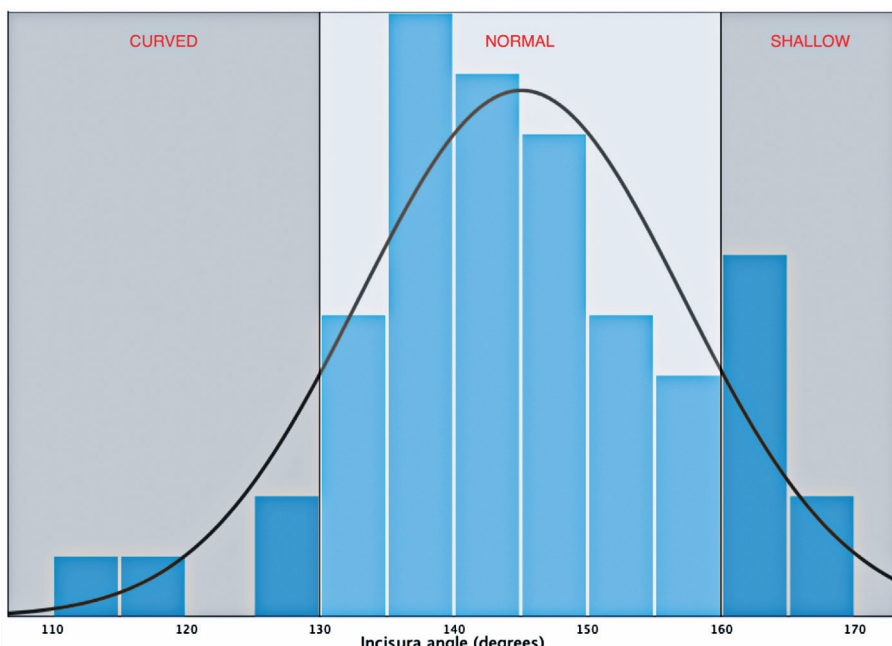


Figure 2. Distribution of the incisura angle parameter.

Table 1. Measurements of the different parameters for all patients

Characteristic	N	Overall, N = 53	Uninjured, N = 25	Injured, N = 28	p-value
Sex, % (n)	53				0.023
w		36 (19)	20 (5)	50 (14)	
m		64 (34)	80 (20)	50 (14)	
Age (years)	53				0.72
Median [Q1, Q3]		39 [30, 58]	36 [27, 60]	39 [33, 57]	
Mean (SD)		43 (17)	43 (19)	43 (15)	
Side, % (n)	53				0.91
r		53 (28)	52 (13)	54 (15)	
l		47 (25)	48 (12)	46 (13)	
Incisura length (mm)	53				0.030
Median [Q1, Q3]		23.90 [22.50, 25.80]	25.30 [23.20, 26.40]	23.40 [21.90, 24.83]	
Mean (SD)		24.20 (2.28)	24.98 (2.26)	23.51 (2.10)	
Incisura depth (mm)	53				0.26
Median [Q1, Q3]		3.90 [2.80, 4.70]	4.10 [3.20, 4.70]	3.55 [2.60, 4.63]	
Mean (SD)		3.79 (1.36)	3.94 (1.09)	3.65 (1.57)	
Incisura angle (degrees)	53				0.62
Median [Q1, Q3]		144 [137, 152]	142 [137, 151]	145 [137, 155]	
Mean (SD)		145 (12)	144 (10)	145 (14)	
Fibular engagement (mm)	45				0.017
Median [Q1, Q3]		0.90 [-0.30, 1.40]	1.20 [0.60, 1.40]	-0.05 [-0.43, 0.90]	
Mean (SD)		0.66 (1.12)	0.96 (1.03)	0.28 (1.13)	
Unknown		8	0	8	
Sydesmosis anterior length (mm)	45				0.95
Median [Q1, Q3]		3.10 [2.70, 4.20]	3.20 [2.80, 3.90]	2.90 [2.50, 4.78]	
Mean (SD)		3.38 (1.39)	3.27 (1.11)	3.51 (1.69)	
Unknown		8	0	8	
Syndesmosis posterior length (mm)	45				0.34
Median [Q1, Q3]		6.10 [5.10, 7.00]	6.30 [5.20, 7.30]	5.55 [4.98, 6.50]	
Mean (SD)		6.07 (1.62)	6.20 (1.79)	5.92 (1.40)	
Unknown		8	0	8	
Triangle area (mm ²)	53				0.11
Median [Q1, Q3]		47 [34, 57]	52 [39, 57]	41 [30, 53]	
Mean (SD)		46 (17)	49 (14)	43 (20)	
Incisura proportion	53				0.14
Median [Q1, Q3]		2.97 [2.47, 4.39]	2.84 [2.34, 3.78]	3.52 [2.52, 5.02]	
Mean (SD)		3.84 (2.21)	3.31 (1.55)	4.32 (2.61)	
Fx Tibia, % (n)	53				< 0.001
none		58 (31)	100 (25)	21 (6)	
POS		25 (13)	0 (0)	46 (13)	
not dislocated		17 (9)	0 (0)	32 (9)	
dislocated		0 (0)	0 (0)	0 (0)	
Fx Fibula, % (n)	53				< 0.001
none		57 (30)	100 (25)	18 (5)	
POS		28 (15)	0 (0)	54 (15)	
not dislocated		15 (8)	0 (0)	29 (8)	
dislocated		0 (0)	0 (0)	0 (0)	

¹ Pearson's Chi-squared test; Wilcoxon rank sum test; Wilcoxon rank sum exact test; Fisher's exact test.

strong correlation (Pearson's correlation coefficient = -0.87) between the incisura angle and the triangle area ($p < 0.001$).

Fibular engagement

Fibular engagement ranged from -1.6 mm to 3.0 mm, with an average of 0.65 mm ($SD \pm 1.17$ mm). There was a moderate correlation (Pearson's correlation coefficient = 0.52) between the triangle area and the fibular engagement ($p < 0.001$). There was also a moderate correlation (Pearson's correlation coefficient = -0.57) between the incisura angle and the fibular engagement ($p < 0.001$).

Fibular engagement differed significantly between the subgroups of uninjured and injured patients. The average engagement in the uninjured group was 0.96 mm, compared to an average of 0.28 mm in the injured group ($p = 0.017$).

Syndesmosis anterior length

The syndesmosis anterior length ranged from 0.9 mm to 6.9 mm, with an average of 3.37 mm ($SD \pm 1.45$ mm).

Syndesmosis posterior length

The syndesmosis posterior length ranged from 2.4 mm to 10.4 mm, with an average of 6.08 mm ($SD \pm 1.58$ mm).

Discussion

This is the first study to determine the angle of the incisura fibularis in addition to various known parameters of tibiofibular syndesmosis. Our goal was to interpret the measured values to understand which parameters affect the basic properties of the tibiofibular syndesmosis. As some previous studies have shown, different anatomical variants of the incisura fibularis correlate with certain malalignments in the treatment of syndesmosis injuries^(16,17). Having a detailed knowledge of the parameters that define the incisura fibularis and the ability to interpret this data could, however, lead to a better understanding of the treatment of related injuries. It could help identifying syndesmoses at risk for postoperative malreduction, reducing the risk of ankle osteoarthritis.

We therefore suggested a new classification of the tibiofibular syndesmosis using the incisura angle as the defining parameter. The above-described St. Georg Classification of the incisura fibularis used the mean incisura angle (144.60°) and its SD (± 12.01 °). Regarding practicability, round numbers were chosen as cutoffs between the groups. This led to the following classification:

St. Georg Classification of the incisura fibularis:

- Curved incisura fibularis (I_c): every angle < 130°;
- Normal incisura fibularis (I_o): every angle between 130° and 160°; and
- Shallow incisura fibularis (I_s): every angle > 160°.

Future studies need to show the impact of this classification on different injury patterns. We suggest that surgeons

should be particularly aware of potential difficulties when faced with an I_c (risk of operative overcompression) or I_s (risk of operative malreduction) during ankle surgery. A possible approach could be performing intraoperative 3D scans of both ankles if the injured ankle is classified as I_c or I_s on preoperative CT. These 3D scans are known to provide beneficial information^(18,19). However, they also lengthen the operation, so knowing in which patients this additional imaging is most helpful could lead to better results and time and resource management in the operating room⁽²⁰⁾. The non-injured side would serve as a benchmark for the surgical treatment of the injury, although side differences in tibia anatomy have been described⁽²¹⁾. This could help to avoid malreduction when faced with difficult anatomy.

Various studies have previously examined the bony structures of the ankle using different measurements. Chen et al.⁽²²⁾ and Ebinger et al.⁽²³⁾ used complex computerized 3D models to describe anatomical variations. We believe these results provide important insights for research but are not simple enough to be used in clinical practice. Standard CT imaging seems to provide the right balance between complexity and practicality, as this imaging modality is also used for clinical assessment of ankle injuries⁽²⁴⁻²⁷⁾.

However, there are few parameters that are consistently used in many studies and can be considered as the main factors to describe the structure at issue. Elgafy et al.⁽²⁵⁾ focused on the parameters syndesmosis anterior length and syndesmosis posterior length. Dikos et al.⁽²⁴⁾ looked closely to the relationship between tibia and fibula, but did not describe the incisura fibularis properly. The first paper we found comparing the anatomy of the incisura fibularis to malreduction patterns during surgery was the work of Cherney et al.⁽¹⁷⁾, in 2016, as they focused on the incisura depth. In the abovementioned work, a shallow incisura was described as increasing the risk of anterior fibular malreduction. A following study by Boszczyk et al.⁽¹⁶⁾ also looked at the fibular engagement as a possible risk factor. They found that a low preoperative fibular engagement may result in overcompression during surgery. As authors focused on different parameters, it is hard to compare results. Therefore, we hope to contribute to a better understanding of the parameters that should be mandatorily measured in the assessment of syndesmosis injuries. This would lead to more comparable results in future studies.

There is an almost perfect correlation between the incisura angle and the incisura depth (Pearson's correlation coefficient = -0.96). Therefore, one can assume that different angles of the incisura could also lead to different malreduction patterns. Further studies should show whether the incisura angle has significant influence on treatments of syndesmotic injuries. We believe this angle can serve as a vivid parameter to describe the incisura fibularis, as it is more easily pictured than depth, only differing in the millimeters.

Looking especially at the fibular engagement, we found that the uninjured group showed significantly higher fibular engagement than the injured group. This can be explained by the concomitant injuries of an ankle fracture. In addition

to bony injuries, ligament and soft tissue injuries can also occur⁽²⁸⁻³⁰⁾. Injuries to the tibiofibular syndesmosis ligaments, in particular, widen the tibiofibular gap and therefore have an influence on the fibular engagement parameter⁽¹¹⁾. The positional shift of the fibula in relation to the tibia and the talocrural joint in the coronal plane is known to raise the probability of chronic ankle instability⁽³¹⁻³³⁾. Furthermore, malreduction of the fibula may lead to high pressure zones in ankle cartilage, which eventually favors arthritis^(34,35). Again, future studies should evaluate the influence of fibular engagement on long term morbidity.

The triangle area is a reliable parameter to combine the parameters incisura length, incisura depth and incisura angle. It roughly represents the size of the articular surface of the fibula. Therefore, this parameter could serve as a future benchmark when comparing the bony structure of ankles in scientific papers. As this parameter is more difficult to picture and cannot be quickly measured, the triangle area would probably be of lower value in clinical use. It combines the abovementioned parameters, so that one can describe the anatomy with four instead of six parameters.

Figure 3 shows the correlations between the triangle area, fibular engagement, syndesmosis anterior length, and syndesmosis posterior length.

Comparing our results to those of other studies, Cherney et al.⁽¹⁷⁾ subdivided their patients considering the incisura depth, although that subdivision was made somehow artificial, as the cutoffs were randomly chosen. The authors defined the group average incisura depth as presenting a depth of 3.5 mm \pm 1 mm. This is consistent with our measurements of the incisura depth, whose average is 3.79 mm. Their subdivision goes back to a 2002 magnetic resonance imaging study by Mavi et al.⁽³⁶⁾, which examined 18 patients, and a 2009 study by Taser et al.⁽³⁷⁾ that measured distances on 35 cadavers. We believe our study presented consistent data of different parameters of the incisura fibularis for surgeons and other physicians to work with in the future.

There is a medium correlation between the triangle area and fibular engagement (Pearson's correlation coefficient = 0.56). This suggests that a bigger articular surface of the fibula correlates with the fibula being more compressed towards the tibia. In opposition, a shallow incisura correlates with a fibula that is not that protected by tibial structures. When confronted with a fractured fibula, it can be challenging to replace the bone back in its anatomical position^(13,38-40). This paper suggests that it is possible to see the shape of the incisura fibularis as a reference for the original position of the fibula. This knowledge could help surgeons to better evaluate

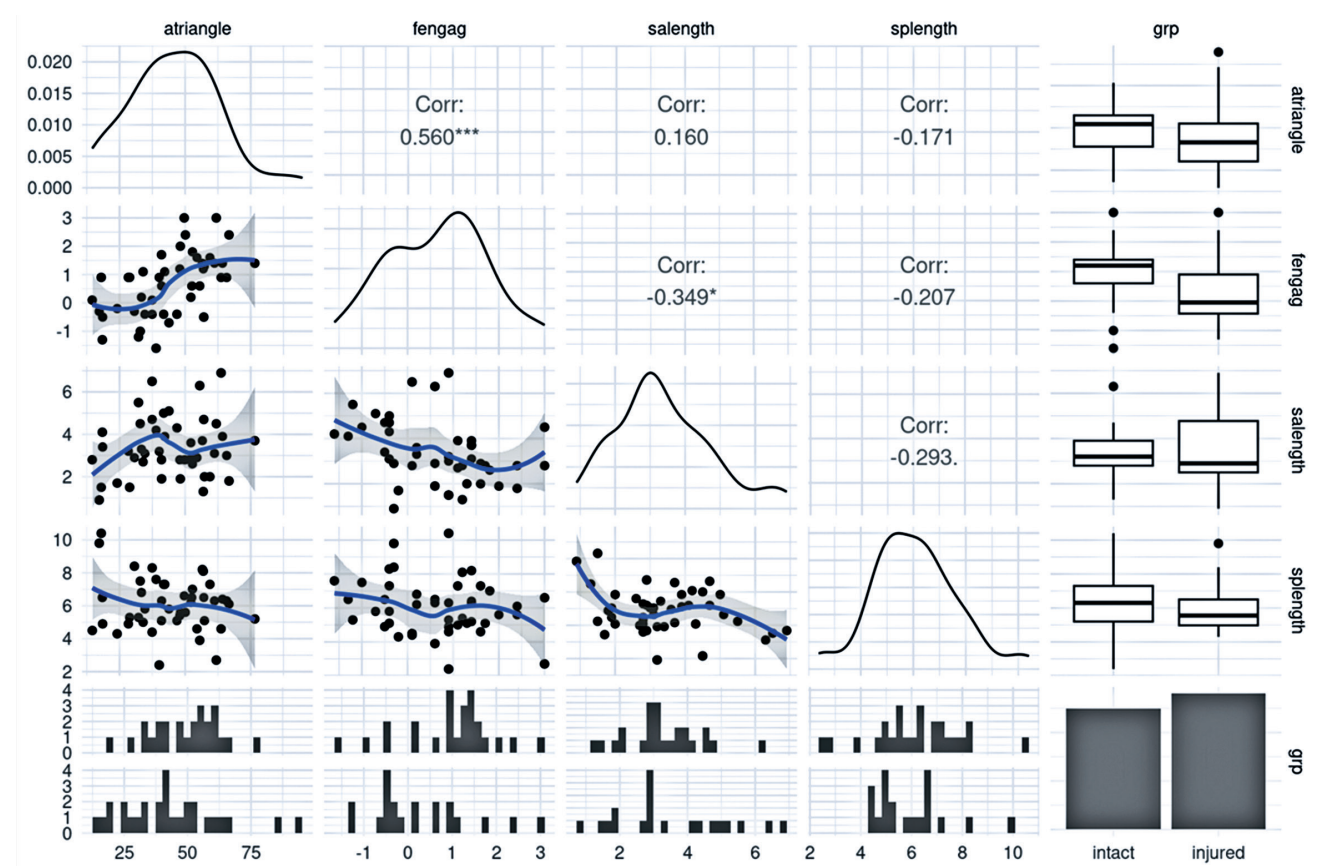


Figure 3. Correlations between triangle area, fibular engagement, syndesmosis anterior length, and syndesmosis posterior length.

anatomical variations prior to ankle surgery to achieve anatomical reduction.

The difference between the average length of the incisura fibularis in both subgroups is most likely due to the different proportion of male patients in such subgroups. Men also have larger bones than women due to their larger body size^[41,42]. Since 80% of the patients in the uninjured subgroup were male, it is plausible that the average length of the incisure is therefore also greater than in the “injured” subgroup, in which the proportion of male patients was 50%. We therefore cannot assume that the incisura length has an influence on the probability of injury.

This study is limited by the small number of patients. Especially when comparing subgroups, the numbers become relatively small. Future, bigger studies will be necessary to strengthen the correlations found in this work. Additionally, injuries on CT imaging never look the same. We were able

to define groups by looking at the injury patterns, but interindividual differences remain and cannot be fully excluded.

We performed measurements 10 mm above the tibiotalar joint gap, as several other studies have done previously^[24,25,43,44]. This helps achieving results comparable with the literature; however, differences in patients’ height were not considered.

Conclusion

This is the first study to suggest that the angle of the tibiofibular syndesmosis can serve as a classification parameter to subdivide anatomical variants. Future studies should investigate whether these variants are correlated with specific injury and malreduction patterns. In addition, this study provides coherent reference data for all parameters defining tibiofibular syndesmosis compared with previous studies.

Authors' contributions: Each author contributed individually and significantly to the development of this article: NB *(<https://orcid.org/0009-0006-2651-3711>) Conceived and planned the activities that led to the study, data collection, statistical analysis, bibliographic review, interpreted the results of the study, and formatting of the article; HG *(<https://orcid.org/0009-0004-5686-1317>) Interpreted the results of the study and participated in the review process; MF *(<https://orcid.org/0000-0002-4123-2903>) Conceived and planned the activities that led to the study, interpreted the results of the study, and participated in the review process. All authors read and approved the final manuscript. *ORCID (Open Researcher and Contributor ID) .

References

1. Khambete P, Harlow E, Ina J, Miskovsky S. Biomechanics of the Distal Tibiofibular Syndesmosis: A Systematic Review of Cadaveric Studies. *Foot Ankle Orthop.* 2021;6(2):24730114211012701.
2. Yuen CP, Lui TH. Distal Tibiofibular Syndesmosis: Anatomy, Biomechanics, Injury and Management. *Open Orthop J.* 2017; 11:670-7.
3. Hermans JJ, Beumer A, de Jong TA, Kleinrensink GJ. Anatomy of the distal tibiofibular syndesmosis in adults: a pictorial essay with a multimodality approach. *J Anat.* 2010;217(6):633-45.
4. Herzog MM, Kerr ZY, Marshall SW, Wikstrom EA. Epidemiology of Ankle Sprains and Chronic Ankle Instability. *J Athl Train.* 2019;54(6):603-10.
5. Waterman BR, Owens BD, Davey S, Zaccagnini MA, Belmont PJ, Jr. The epidemiology of ankle sprains in the United States. *J Bone Joint Surg Am.* 2010;92(13):2279-84.
6. Hunt KJ, Phisitkul P, Pirolo J, Amendola A. High Ankle Sprains and Syndesmotic Injuries in Athletes. *J Am Acad Orthop Surg.* 2015;23(11):661-73.
7. Hunt KJ, George E, Harris AH, Dragoo JL. Epidemiology of syndesmosis injuries in intercollegiate football: incidence and risk factors from National Collegiate Athletic Association injury surveillance system data from 2004-2005 to 2008-2009. *Clin J Sport Med.* 2013;23(4):278-82.
8. Waterman BR, Belmont PJ, Jr., Cameron KL, Svoboda SJ, Alitz CJ, Owens BD. Risk factors for syndesmotic and medial ankle sprain: role of sex, sport, and level of competition. *Am J Sports Med.* 2011;39(5):992-8.
9. Press CM, Gupta A, Hutchinson MR. Management of ankle syndesmosis injuries in the athlete. *Curr Sports Med Rep.* 2009;8(5):228-33.
10. Porter DA, Jagers RR, Barnes AF, Rund AM. Optimal management of ankle syndesmosis injuries. *Open Access J Sports Med.* 2014;5:173-82.
11. Cornu O, Manon J, Tribak K, Putineanu D. Traumatic injuries of the distal tibiofibular syndesmosis. *Orthop Traumatol Surg Res.* 2021;107(1s):102778.
12. de-Las-Heras Romero J, Alvarez AML, Sanchez FM, Garcia AP, Porcel PAG, Sarabia RV, et al. Management of syndesmotic injuries of the ankle. *EFORT Open Rev.* 2017;2(9):403-9.
13. Gardner MJ, Demetrakopoulos D, Briggs SM, Helfet DL, Lorich DG. Malreduction of the tibiofibular syndesmosis in ankle fractures. *Foot Ankle Int.* 2006;27(10):788-92.
14. Kaftandziev I, Bakota B, Trpeski S, Arsovski O, Spasov M, Cretnik A. The effect of the ankle syndesmosis reduction quality on the short-term functional outcome following ankle fractures. *Injury.* 2021;52(Suppl 5):S70-s4.

15. Sagi HC, Shah AR, Sanders RW. The functional consequence of syndesmotic joint malreduction at a minimum 2-year follow-up. *J Orthop Trauma*. 2012;26(7):439-43.
16. Boszczyk A, Kwapisz S, Krümmel M, Grass R, Rammelt S. Correlation of Incisura Anatomy With Syndesmotic Malreduction. *Foot Ankle Int*. 2018;39(3):369-75.
17. Cherney SM, Spraggs-Hughes AG, McAndrew CM, Ricci WM, Gardner MJ. Incisura Morphology as a Risk Factor for Syndesmotic Malreduction. *Foot Ankle Int*. 2016;37(7):748-54.
18. Cunningham BA, Warner S, Berkes M, Achor T, Choo A, Munz J, et al. Effect of Intraoperative Multidimensional Fluoroscopy Versus Conventional Fluoroscopy on Syndesmotic Reduction. *Foot Ankle Int*. 2021;42(2):132-6.
19. Kumar V, Baburaj V, Patel S, Sharma S, Vaishya R. Does the use of intraoperative CT scan improve outcomes in Orthopaedic surgery? A systematic review and meta-analysis of 871 cases. *J Clin Orthop Trauma*. 2021;18:216-23.
20. Richter M, Zech S. Intraoperative 3-dimensional imaging in foot and ankle trauma-experience with a second-generation device (ARCADIS-3D). *J Orthop Trauma*. 2009;23(3):213-20.
21. Quintens L, Herteleer M, Vancleef S, Carette Y, Duflou J, Nijs S, et al. Anatomical Variation of the Tibia - a Principal Component Analysis. *Sci Rep*. 2019;9(1):7649.
22. Chen Y, Qiang M, Zhang K, Li H, Dai H. A reliable radiographic measurement for evaluation of normal distal tibiofibular syndesmosis: a multi-detector computed tomography study in adults. *J Foot Ankle Res*. 2015;8:32.
23. Ebinger T, Goetz J, Dolan L, Phisitkul P. 3D model analysis of existing CT syndesmosis measurements. *Iowa Orthop J*. 2013;33:40-6.
24. Dikos GD, Heisler J, Choplin RH, Weber TG. Normal tibiofibular relationships at the syndesmosis on axial CT imaging. *J Orthop Trauma*. 2012;26(7):433-8.
25. Elgafy H, Semaan HB, Blessinger B, Wassef A, Ebraheim NA. Computed tomography of normal distal tibiofibular syndesmosis. *Skeletal Radiol*. 2010;39(6):559-64.
26. Tourné Y, Molinier F, Andrieu M, Porta J, Barbier G. Diagnosis and treatment of tibiofibular syndesmosis lesions. *Orthop Traumatol Surg Res*. 2019;105(8s):275-86.
27. van Zuuren WJ, Schepers T, Beumer A, Sierevelt I, van Noort A, van den Bekerom MPJ. Acute syndesmotic instability in ankle fractures: A review. *Foot Ankle Surg*. 2017;23(3):135-41.
28. Lee S, Lin J, Hamid KS, Bohl DD. Deltoid Ligament Rupture in Ankle Fracture: Diagnosis and Management. *J Am Acad Orthop Surg*. 2019;27(14):e648-e58.
29. Wake J, Martin KD. Syndesmosis Injury From Diagnosis to Repair: Physical Examination, Diagnosis, and Arthroscopic-assisted Reduction. *J Am Acad Orthop Surg*. 2020;28(13):517-27.
30. Goost H, Wimmer MD, Barg A, Kabir K, Valderrabano V, Burger C. Fractures of the ankle joint: investigation and treatment options. *Dtsch Arztebl Int*. 2014;111(21):377-88.
31. Scranton PE, Jr., McDermott JE, Rogers JV. The relationship between chronic ankle instability and variations in mortise anatomy and impingement spurs. *Foot Ankle Int*. 2000;21(8):657-64.
32. McDermott JE, Scranton PE, Jr., Rogers JV. Variations in fibular position, talar length, and anterior talofibular ligament length. *Foot Ankle Int*. 2004;25(9):625-9.
33. Bonnel F, Toullec E, Mabit C, Tourné Y. Chronic ankle instability: biomechanics and pathomechanics of ligaments injury and associated lesions. *Orthop Traumatol Surg Res*. 2010;96(4):424-32.
34. Dahmen J, Karlsson J, Stufkens SAS, Kerkhoffs G. The ankle cartilage cascade: incremental cartilage damage in the ankle joint. *Knee Surg Sports Traumatol Arthrosc*. 2021;29(11):3503-7.
35. Anderson DD, Marsh JL, Brown TD. The pathomechanical etiology of post-traumatic osteoarthritis following intraarticular fractures. *Iowa Orthop J*. 2011;31:1-20.
36. Mavi A, Yildirim H, Gunes H, Pestamalci T, Gümüşburun E. The fibular incisura of the tibia with recurrent sprained ankle on magnetic resonance imaging. *Saudi Med J*. 2002;23(7):845-9.
37. Taşer F, Toker S, Kılıنçoğlu V. Evaluation of morphometric characteristics of the fibular incisura on dry bones. *Eklem Hastalik Cerrahisi*. 2009;20(1):52-8.
38. Stenquist DS, Kwon JY. Strategies to Avoid Syndesmosis Malreduction in Ankle Fractures. *Foot Ankle Clin*. 2020;25(4):613-30.
39. Githens MF, DeBaun MR, Jacobsen KA, Ross H, Firoozabadi R, Haller J. Plafond Malreduction and Talar Dome Impaction Accelerates Arthrosis After Supination-Adduction Ankle Fracture. *Foot Ankle Int*. 2021;42(10):1245-53.
40. Futamura K, Baba T, Mogami A, Morohashi I, Kanda A, Obayashi O, et al. Malreduction of syndesmosis injury associated with malleolar ankle fracture can be avoided using Weber's three indexes in the mortise view. *Injury*. 2017;48(4):954-9.
41. Chun DI, Cho JH, Yi Y, Kim J, Park SY, Kim JH, et al. A Novel Model for Predicting the Sagittal Length of the Distal Tibia Using CT Imaging and Statistics. *J Foot Ankle Surg*. 2024;63(2):132-5.
42. Sahin R, Şahin S, Kazdal C, Balık MS. Can the Length of the Tibia Nail Be Predicted Correctly Before the Operation According to the Patient's Height and Shoe Size? *Cureus*. 2024;16(1):e52653.
43. Ebraheim NA, Lu J, Yang H, Rollins J. The fibular incisure of the tibia on CT scan: a cadaver study. *Foot Ankle Int*. 1998;19(5):318-21.
44. Mendelsohn ES, Hoshino CM, Harris TG, Zinar DM. CT characterizing the anatomy of uninjured ankle syndesmosis. *Orthopedics*. 2014;37(2):e157-60.